Journal of Mathematical Chemistry 25 (1999) 7–21

Symmetry breaking in HF wave functions of $Fe(CH)_2$

Maria Jaworska and Piotr Lodowski

Department of Theoretical Chemistry, Silesian University, Szkolna 9, PL-40006 Katowice, Poland
E-mail: mj@tc3.ich.us.edu.pl

Received 23 July 1997; revised 20 October 1998

HF and CAS calculations for linear geometry of $Fe(CH)_2$ with $D_{\infty h}$ symmetry have been performed. The basis sets used were DZ and DZ + P with ECP on the iron atom. Two closed-shell and one quintet RHF wave functions have been found, Φ_1^{RHF}, Φ_2^{RHF} and $\Phi_3^{RHF(Q)}$. All of them are singlet and triplet unstable in the wide range of Fe–CH distances. Singlet instability leads to the Charge Density Wave (CDW) broken-symmetry wave function with two electrons on carbon p_x or p_y orbital in the dissociation limit. Triplet instabilities lead to two broken-symmetry HF wave functions of Axial Spin Density Wave (ASDW) type, $ASDW_1$ and $ASDW_2$. In the dissociation limit they give carbon atoms with two electrons on p_x and p_y orbitals coupled to singlet and triplet, respectively. The stability conditions for CDW, $ASDW_1$ and $ASDW_2$ instabilities have been derived. Other HF wave functions with spin symmetry unrestricted have been also found. CAS(8,8), CAS(10,10) and CAS(12,12) calculations for singlet, triplet and quintet states of $Fe(CH)_2$ have been carried out. In all CAS calculations the singlet state has the lowest energy. The Fe–CH equilibrium distances obtained from closed-shell RHF wave functions are much shorter and from broken-symmetry wave functions are much longer than those obtained from CAS calculations.

1. Introduction

The Hartree–Fock equations are nonlinear equations, and, consequently, they can have more than one solution. In some cases there exist HF wave functions of lower symmetry than that of the molecule and of lower energy than energy corresponding to the symmetry adapted RHF wave function. This phenomenon was called "the symmetry dilemma" by Löwdin [46]. Slater showed [73] that for the large interatomic distances in the hydrogen molecule the broken-symmetry wave function is lower in energy than the symmetric one. The occurrence of symmetry breaking is a sign that correlation effects are important in the system. All types of HF solutions were classified by Fukutome [28–30,61] according to the various symmetry groups. When a symmetry broken wave function exists, the RHF symmetry adapted wave function is unstable (it is not a minimum in the variational space). HF instabilities occur in singly bonded systems for large interatomic distances. The HF instabilities for cyclic and linear polyenes were extensively studied and the stability conditions for these systems were derived [63–70,75]. The class of molecules for which the wave functions are unstable

at the equilibrium atom–atom distance are molecules with multiple bonds [22,39–41], linear carbon clusters [44], systems with metal–metal bonds and organometallic molecules [4,10–14,17–19,21,23,33,37,55,77,78]. HF calculations for one-dimensional metals lead to spin density wave (UHF) and charge density wave (RHF) soutions [49,50]. HF instabilities are also relevant to the description of hole states in molecules [1,5,6,16]. The broken-symmetry method has been designed and used with significant success to interpret magnetic and spectroscopic properties of biologically important systems and transition metal dimers [7,34,45,51,54,56–60,72,82,84]. The HF instabilities appear in reactive systems, transition states of reactions, unstable intermediates and other systems with unusal electronic properties [76,79–81,83,85]. Instabilities occur also in DFT calculations but they are less pronounced than HF instabilities, which is related to effects of electron correlation included in the DFT correlation potentials [32]. Symmetry breaking plays also a role in CC, MCSCF and perturbation theory calculations [3,31,38,42,43,52,74]. The different aspects of symmetry breaking in atoms and molecules and the HF stability related problems are reviewed in [20,30,53,62].

In this work we have studied the HF instabilities for the model organometallic molecule bis(methyne)iron, $Fe(CH)_2$. We have examined instabilities which localize different pairs of electrons in different parts of the molecule, that is, singlet instabilities leading to Charge Density Wave (CDW) broken-symmetry solutions, and instabilities localizing electrons of different spins in different parts of the molecule, that is, triplet instabilities leading to Axial Spin Density Wave (ASDW) broken-symmetry solutions.

2. Method of calculations

The calculations have been carried out with the GAMESS program [25]. The valence double-ζ basis of Dunning and Huzinaga [8,24] has been used for carbon and hydrogen atoms. The core electrons of Fe have been replaced by an effective core potential [36] and the basis set of DZ quality of Hay and Wadt [36] has been used for valence electrons. This basis, which is further referred to as B_1 has been used in all HF calculations. We subsequently performed some HF calculations and CAS calculations with two basis sets. The first was B_1 and the second, B_2, was formed by adding one polarization p function on the hydrogen with exponent 1.0, one polarization d function on the carbon with exponent 0.75, and one additional diffuse d function on the iron atom [35].

The linear structure of $D_{\infty h}$ symmetry was assumed for $Fe(CH)_2$. The energy curves have been determined for different distances of Fe–CH, equal for both ligands.

3. Results and discussion

$Fe(CH)_2$ can be considered as a result of ethyne dissociation with Fe atom participation as a catalyst. The ligated carbyne and bis(carbyne) complexes of transition

metals are known [2,15,26,27,47,48,71]. The high symmetry of the linear $Fe(CH)_2$ molecule permits facile investigation of the symmetry properties and symmetry breaking in the HF wave functions of this system.

3.1. HF wave functions for Fe(CH)$_2$

We started from the closed-shell RHF calculations. The usual iterative procedure leads to a solution which we denote Φ_1^{RHF}. From among nine MOs occupied by eighteen valence electrons, the two lowest σ_g and σ_u describe plus and minus combinations of $\sigma_{\mathrm{C–H}}$ and are common to all HF wave functions found. They can be omitted from further considerations. The HF determinant for the remaining seven MOs is

$$\Phi_1^{\mathrm{RHF}} = \left|1\sigma_g^2(p_{zC})1\sigma_u^2(p_{zC})d_{xy}^2 d_{x^2-y^2}^2 2\sigma_g^2(d_{z^2})\pi_{xg}^2\pi_{yg}^2\right|, \tag{3.1.1}$$

where

$$\pi_{xg} = ad_{xz} + b(p_{xC_A} - p_{xC_B}), \tag{3.1.2}$$

$$\pi_{yg} = ad_{yz} + b(p_{yC_A} - p_{yC_B}). \tag{3.1.3}$$

Coefficients a and b are here 0.27 and 0.38, respectively (these are coefficients for the first function of the double-ζ basis). There is a significant admixture of d_{z^2} orbital to $1\sigma_g$ orbital and of p_z orbitals of carbon to $2\sigma_g$ orbital for this wave function.

Φ_1^{RHF} is unstable, leading to three broken-symmetry solutions, one of CDW and two of ASDW type:

$$\Phi_1^{\mathrm{CDW}} = \left|1\sigma_g^2(p_{zC})1\sigma_u^2(p_{zC})d_{xy}^2 d_{x^2-y^2}^2 2\sigma_g^2(d_{z^2})\pi_{xA}^2\pi_{yB}^2\right|, \tag{3.1.4}$$

$$\Phi_1^{\mathrm{ASDW_1}} = \left|1\sigma_g^2(p_{zC})1\sigma_u^2(p_{zC})d_{xy}^2 d_{x^2-y^2}^2 2\sigma_g^2(d_{z^2})\pi_{xA}\bar{\pi}_{yA}\bar{\pi}_{xB}\pi_{yB}\right|, \tag{3.1.5}$$

$$\Phi_1^{\mathrm{ASDW_2}} = \left|1\sigma_g^2(p_{zC})1\sigma_u^2(p_{zC})d_{xy}^2 d_{x^2-y^2}^2 2\sigma_g^2(d_{z^2})\pi_{xA}\pi_{yA}\bar{\pi}_{xB}\bar{\pi}_{yB}\right|. \tag{3.1.6}$$

The energy as a function of the Fe–CH distance for Φ_1^{RHF}, Φ_1^{CDW}, $\Phi_1^{\mathrm{ASDW_1}}$ and $\Phi_1^{\mathrm{ASDW_2}}$ solutions is shown in figure 1. The π orbitals in these three wave functions are localized on atomic orbitals of different carbon atoms which can be visualized in a simple way (cf. scheme 1). At shorter Fe–CH distances localization is not complete, the π_{xA} and π_{yA} orbitals have tails on carbon B and vice versa. This localization takes place at a very short Fe–C distance, much shorter than the minimum energy distance of Φ_1^{RHF} (figure 1).

There is another closed shell RHF wave function, Φ_2^{RHF}, which is lower in energy than Φ_1^{RHF}. The respective determinant formed from the seven highest occupied MOs is

$$\Phi_2^{\mathrm{RHF}} = \left|d_{xy}^2 d_{xz}^2 d_{yz}^2 \sigma_g^2(p_{zC})\sigma_u^2(p_{zC})\pi_{xu}^2\pi_{yu}^2\right|, \tag{3.1.7}$$

where, after ommiting normalization,

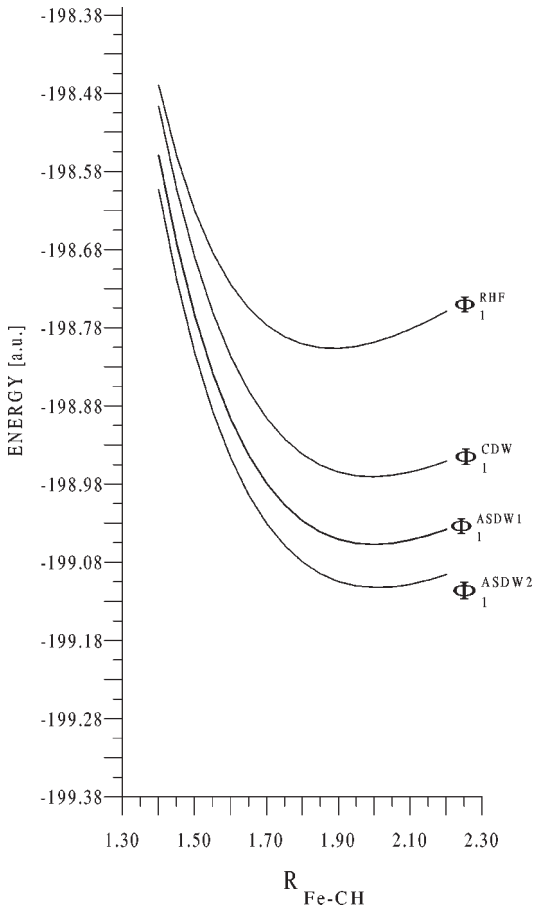

Figure 1. Energy curves for Φ_1^{RHF} and broken-symmetry solutions Φ_1^{CDW}, $\Phi_1^{\text{ASDW}_1}$ and $\Phi_1^{\text{ASDW}_2}$.

$$\pi_{xu} = p_{xC_A} + p_{xC_B}, \tag{3.1.8}$$

$$\pi_{yu} = p_{yC_A} + p_{yC_B}. \tag{3.1.9}$$

This wave function is also unstable. We get three broken-symmetry solutions arising from Φ_2^{RHF} similar to those for Φ_1^{RHF}:

$$\Phi_2^{\text{CDW}} = \left| d_{xy}^2 d_{xz}^2 d_{yz}^2 \sigma_g^2(p_{zC}) \sigma_u^2(p_{zC}) \pi_{xA}^2 \pi_{yB}^2 \right|, \tag{3.1.10}$$

$$\Phi_2^{\text{ASDW}_1} = \left| d_{xy}^2 d_{xz}^2 d_{yz}^2 \sigma_g^2(p_{zC}) \sigma_u^2(p_{zC}) \pi_{xA} \bar{\pi}_{yA} \bar{\pi}_{xB} \pi_{yB} \right|, \tag{3.1.11}$$

$$\Phi_2^{\text{ASDW}_2} = \left| d_{xy}^2 d_{xz}^2 d_{yz}^2 \sigma_g^2(p_{zC}) \sigma_u^2(p_{zC}) \pi_{xA} \pi_{yA} \bar{\pi}_{xB} \bar{\pi}_{yB} \right|. \tag{3.1.12}$$

Again the π orbitals are localized on different carbon atoms in the way described in scheme 1. The $\sigma(p_{zC})$ orbitals can be localized by transformation between σ_g and σ_u occupied orbitals. Such transformation does not cause an energy change and

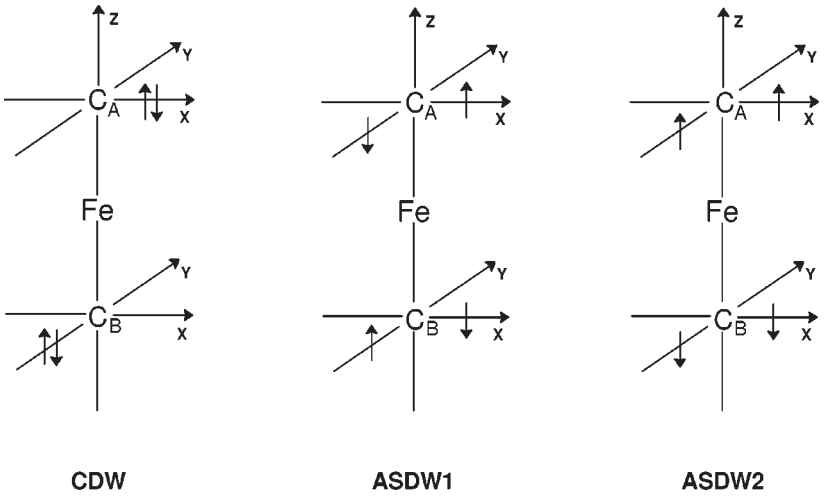

Scheme 1.

symmetry breaking. The energy curves for Φ_2^{RHF} and the broken-symmetry wave functions arising from it as functions of the Fe–CH distance are shown in figure 2.

The localization starts at a very short Fe–CH distance, like in the case of the wave function Φ_1^{RHF}. The broken-symmetry wave functions arising from Φ_1^{RHF} and Φ_2^{RHF} will dissociate to CH groups with different C atom configurations (p_x^2 or p_y^2 for CDW, $\bar{p}_x p_y$ or $p_x \bar{p}_y$ for ASDW_1 and $p_x p_y$ for ASDW_2) and to the high-energy atomic states Fe atom, due to closed-shell d orbitals occupation. We calculated the RHF wave function in which the Fe atom has four unpaired electrons:

$$\Phi_3^{\mathrm{RHF(Q)}} = \left| d_{z^2} d_{xz} d_{yz} d_{xy} d_{x^2-y^2}^2 \sigma_g^2(p_{zC}) \sigma_u^2(p_{zC}) \pi_{xg}^2 \pi_{yg}^2 \right|, \tag{3.1.13}$$

where π_{xg} and π_{yg} are similar as for Φ_1^{RHF}, but with considerably smaller coefficients on d orbitals ($a = 0.17,\ b = 0.43$). As in the case of Φ_1^{RHF} and Φ_2^{RHF}, π orbitals localize on different carbon atoms giving three broken-symmetry wave functions CDW, ASDW_1 and ASDW_2:

$$\Phi_3^{\mathrm{CDW}} = \left| d_{z^2} d_{xz} d_{yz} d_{xy} d_{x^2-y^2}^2 \sigma_g^2(p_{zC}) \sigma_u^2(p_{zC}) \pi_{xA}^2 \pi_{yB}^2 \right|, \tag{3.1.14}$$

$$\Phi_3^{\mathrm{ASDW_1}} = \left| d_{z^2} d_{xz} d_{yz} d_{xy} d_{x^2-y^2}^2 \sigma_g^2(p_{zC}) \sigma_u^2(p_{zC}) \pi_{xA} \bar{\pi}_{yA} \bar{\pi}_{xB} \pi_{yB} \right|, \tag{3.1.15}$$

$$\Phi_3^{\mathrm{ASDW_2}} = \left| d_{z^2} d_{xz} d_{yz} d_{xy} d_{x^2-y^2}^2 \sigma_g^2(p_{zC}) \sigma_u^2(p_{zC}) \pi_{xA} \pi_{yA} \bar{\pi}_{xB} \bar{\pi}_{yB} \right|. \tag{3.1.16}$$

The energy of $\Phi_3^{\mathrm{RHF(Q)}}$ and broken-symmetry wave functions originating from it as a function of the Fe–CH distance is shown in figure 3. It was not possible to find the energy of CDW and ASDW_1 solutions for smaller Fe–CH distances in this case, because of convergency problems.

Symmetry-broken molecular orbitals for Φ_1^{RHF}, Φ_2^{RHF} and $\Phi_3^{\mathrm{RHF(Q)}}$ can be defined as a combination of occupied and virtual RHF orbitals:

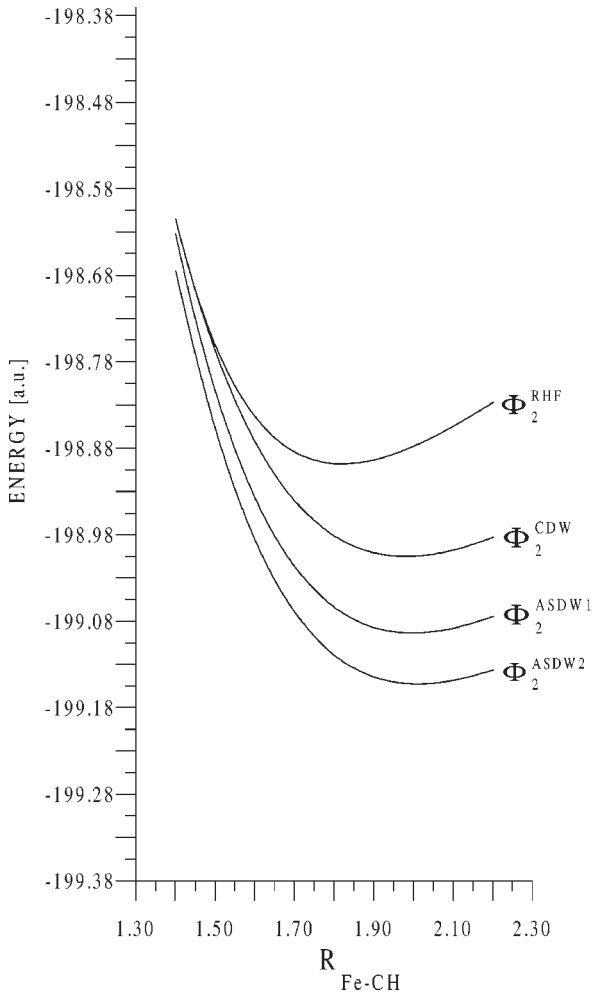

Figure 2. Energy curves for Φ_2^{RHF} and broken-symmetry solutions Φ_2^{CDW}, $\Phi_2^{\mathrm{ASDW_1}}$ and $\Phi_2^{\mathrm{ASDW_2}}$.

$$\text{CDW:}\quad \begin{aligned} \pi_{xA} &= \cos\lambda\pi_{xg(u)} + \sin\lambda\pi^*_{xu(g)},\\ \bar{\pi}_{xA} &= \cos\lambda\bar{\pi}_{xg(u)} + \sin\lambda\bar{\pi}^*_{xu(g)},\\ \pi_{yB} &= \cos\lambda\pi_{yg(u)} - \sin\lambda\pi^*_{yu(g)},\\ \bar{\pi}_{yB} &= \cos\lambda\bar{\pi}_{yg(u)} - \sin\lambda\bar{\pi}^*_{yu(g)}, \end{aligned} \tag{3.1.17}$$

$$\text{ASDW}_1\text{:}\quad \begin{aligned} \pi_{xA} &= \cos\lambda\pi_{xg(u)} + \sin\lambda\pi^*_{xu(g)},\\ \bar{\pi}_{xB} &= \cos\lambda\bar{\pi}_{xg(u)} - \sin\lambda\bar{\pi}^*_{xu(g)},\\ \bar{\pi}_{yA} &= \cos\lambda\bar{\pi}_{yg(u)} + \sin\lambda\bar{\pi}^*_{yu(g)},\\ \pi_{yB} &= \cos\lambda\pi_{yg(u)} - \sin\lambda\pi^*_{yu(g)}, \end{aligned} \tag{3.1.18}$$

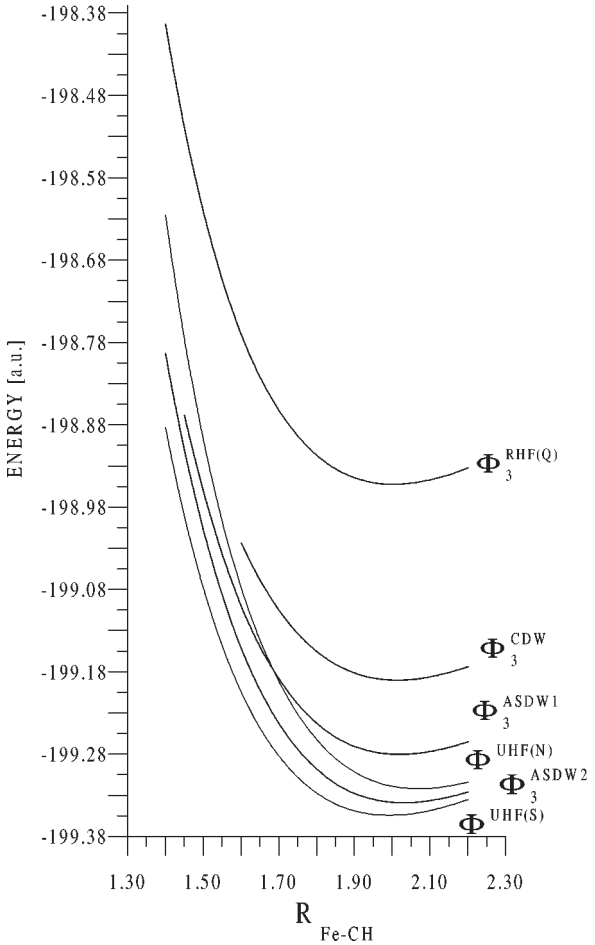

Figure 3. Energy curves for $\Phi_3^{\mathrm{RHF(Q)}}$ and broken-symmetry solutions Φ_3^{CDW}, $\Phi_3^{\mathrm{ASDW_1}}$ and $\Phi_3^{\mathrm{ASDW_2}}$, together with energy curves for $\Phi^{\mathrm{UHF(N)}}$ and $\Phi^{\mathrm{UHF(S)}}$.

$$\begin{aligned} \mathrm{ASDW_2}: \quad \pi_{xA} &= \cos\lambda\pi_{xg(u)} + \sin\lambda\pi^*_{xu(g)}, \\ \bar{\pi}_{xB} &= \cos\lambda\bar{\pi}_{xg(u)} - \sin\lambda\bar{\pi}^*_{xu(g)}, \\ \pi_{yA} &= \cos\lambda\pi_{yg(u)} + \sin\lambda\pi^*_{yu(g)}, \\ \bar{\pi}_{yB} &= \cos\lambda\bar{\pi}_{yg(u)} - \sin\lambda\bar{\pi}^*_{yu(g)}, \end{aligned} \tag{3.1.19}$$

where the subscripts in parentheses correspond to the wave function Φ_2^{RHF} with π_u orbitals occupied. The transformation between virtual orbitals and occupied orbitals leads to localization and considerable lowering of energy for the three wave functions Φ_1^{RHF}, Φ_2^{RHF}, $\Phi_3^{\mathrm{RHF(Q)}}$. At the dissociation limit, $\cos\lambda = \sin\lambda$ and $\lambda = \pi/4$.

In the case when π_{xg} and π_{xu} orbitals were all occupied the transformation of the type (3.1.17)–(3.1.19) would occur between occupied orbitals and would not lead to symmetry breaking. We calculated the energy for several HF wave functions with four

Table 1
Calculated energies, Fe–CH distances (R_{eq}) and $\langle \widehat{S}^2 \rangle$ values for HF wave functions.

Wave function	R_{eq} [Å]	E [a.u.]	$\langle \widehat{S}^2 \rangle$
	Basis B_1		
Φ_1^{RHF}	1.89	−198.806	0
Φ_1^{CDW}	1.99	−198.970	0
$\Phi_1^{ASDW_1}$	1.99	−199.057	1.99
$\Phi_1^{ASDW_2}$	2.01	−199.112	2.03
Φ_2^{RHF}	1.82	−198.898	0
Φ_2^{CDW}	1.98	−199.005	0
$\Phi_2^{ASDW_1}$	1.99	−199.093	1.97
$\Phi_2^{ASDW_2}$	2.01	−199.153	2.03
$\Phi_3^{RHF(Q)}$	2.00	−198.952	6.02
Φ_3^{CDW}	2.01	−199.190	6.02
$\Phi_3^{ASDW_1}$	2.02	−199.280	7.91
$\Phi_3^{ASDW_2}$	2.03	−199.339	7.98
$\Phi^{UHF(N)}$	2.07	−199.322	20
$\Phi^{UHF(S)}$	1.99	−199.354	3.91
	Basis B_2		
$\Phi^{UHF(S)}$	1.98	−199.377	3.91

π orbitals having the same spin. The limiting cases are $\Phi^{UHF(S)}$ with equal number of alpha and beta electrons (formally singlet, but the wave function does not have the correct $\langle \widehat{S}^2 \rangle$ value) and $\Phi^{UHF(N)}$ with eight unpaired alpha electrons. The occupation of molecular orbitals for these two wave functions is

$$\Phi^{UHF(S)} = \left| d_{xy} d_{xz} d_{yz} d_{z^2} d^2_{x^2-y^2} \sigma_g^2(p_{zC}) \sigma_u^2(p_{zC}) \bar{\pi}_{xg} \bar{\pi}_{yg} \bar{\pi}_{xu} \bar{\pi}_{yu} \right|, \quad (3.1.20)$$

and

$$\Phi^{UHF(N)} = \left| d_{xy} d_{xz} d_{yz} d_{z^2} d^2_{x^2-y^2} \sigma_g^2(p_{zC}) \sigma_u^2(p_{zC}) \pi_{xg} \pi_{yg} \pi_{xu} \pi_{yu} \right|, \quad (3.1.21)$$

where $\Phi^{UHF(S)}$ is a spin unrestricted wave function. The $\langle \widehat{S}^2 \rangle$ value for the minimum distance Fe–CH is 3.91 (table 1) which differs significantly from the 0 value for singlet wave functions. The energy curves for $\Phi^{UHF(S)}$ and $\Phi^{UHF(N)}$ are also shown in figure 3.

We have tried other spin couplings leading to two, four and six unpaired electrons for one-determinantal wave function, but in each case the obtained energy was higher than that of $\Phi^{UHF(S)}$. The energy and the Fe–CH distance for calculated HF wave functions are collected in table 1, and orbital populations and charges are given in table 2. The two lowest energy HF wave functions are $\Phi^{UHF(S)}$ and $\Phi_3^{ASDW_2}$. In general, there are possibly many single-determinantal wave functions for $Fe(CH)_2$ with spatial and/or spin symmetry broken which are close in energy. They lead to different Fe–CH equilibrium distances as it may be seen from table 1.

Table 2
Orbital populations and charges for HF wave functions of $Fe(CH)_2$.

Wave function	Fe orbital populations[a]									Charges		
	d_{z^2}	d_{x^2}	d_{y^2}	d_{xz}	d_{yz}	d_{xy}	s	p	d_{total}	Fe	C	H
Basis B_1												
Φ_1^{RHF}	1.19	1.31	1.31	0.47	0.47	2.00	0.64	−0.07	7.32	0.70	−0.48	0.13
Φ_1^{CDW}	1.30	1.31	1.31	0.17	0.17	2.00	0.61	0.11	6.98	1.04	−0.68	0.16
$\Phi_1^{\text{ASDW}_1}$	1.31	1.31	1.31	0.13	0.13	2.00	0.63	0.06	6.88	1.14	−0.72	0.15
$\Phi_1^{\text{ASDW}_2}$	1.32	1.31	1.31	0.11	0.11	2.00	0.66	0.03	6.85	1.16	−0.72	0.14
Φ_2^{RHF}	0.33	−0.04	−0.04	1.92	1.92	2.00	0.49	0.81	7.39	0.64	−0.48	0.16
Φ_2^{CDW}	0.29	−0.03	−0.03	2.00	2.00	2.00	0.45	0.28	6.96	1.06	−0.70	0.17
$\Phi_2^{\text{ASDW}_1}$	0.29	−0.03	−0.03	2.01	2.01	2.00	0.46	0.16	6.87	1.16	−0.74	0.16
$\Phi_2^{\text{ASDW}_2}$	0.21	−0.04	−0.04	2.01	2.01	2.00	0.48	0.11	6.84	1.18	−0.72	0.13
$\Phi_3^{\text{RHF(Q)}}$	0.76	0.64	0.64	1.21	1.21	2.00	0.48	−0.04	6.90	1.10	−0.72	0.17
Φ_3^{CDW}	0.79	0.64	0.64	1.06	1.06	2.00	0.54	0.19	6.92	1.11	−0.72	0.16
$\Phi_3^{\text{ASDW}_1}$	0.79	0.64	0.64	1.05	1.05	2.00	0.55	0.11	6.83	1.18	−0.75	0.16
$\Phi_3^{\text{ASDW}_2}$	0.80	0.64	0.64	1.04	1.04	2.00	0.56	0.08	6.80	1.20	−0.74	0.14
$\Phi^{\text{UHF(N)}}$	0.83	0.64	0.64	1.02	1.02	2.00	0.53	0.08	6.76	1.26	−0.78	0.15
$\Phi^{\text{UHF(S)}}$	0.78	0.63	0.63	1.07	1.07	2.00	0.59	0.05	6.82	1.18	−0.72	0.13
Basis B_2												
$\Phi^{\text{UHF(S)}}$	0.62	0.61	0.61	1.06	1.06	2.00	0.69	0.07	6.72	1.30	−0.76	0.11

[a] Populations on s and p valence orbitals were summed up.

3.2. The stability condition

For the Hartree–Fock wave function to be stable, the second variation of the energy functional expressed in the form

$$\delta^2 E_{\text{HF}}(\Phi) = \frac{1}{2}\lambda^{+}\mathbf{\Omega}\lambda \tag{3.2.1}$$

must be positive. It means that the instability matrix $\mathbf{\Omega}$ has to be positive definite (that is, has to have all eigenvalues positive). The $\mathbf{\Omega}$ matrix elements for instabilities of real character are given for the singlet instability by [30]

$$\Omega_{ma,nb} = F_{mn}\delta_{ab} - F_{ba}\delta_{mn} + 4(ma|nb) - (mn|ab) - (mb|na), \tag{3.2.2}$$

and for the triplet instability by

$$\Omega_{ma,nb} = F_{mn}\delta_{ab} - F_{ba}\delta_{mn} - (mn|ab) - (mb|na), \tag{3.2.3}$$

where m, n label the virtual orbitals and a, b the occupied ones. F_{mn} are elements of the Fock matrix here, and $(mn|ab)$ are two-electron integrals in Mulliken notation.

3.3. The instability conditions for CDW, ASDW$_1$ and ASDW$_2$ solutions

For π orbitals in Φ_1^{RHF}, Φ_2^{RHF}, $\Phi_3^{\mathrm{RHF(Q)}}$ the instability matrix $\mathbf{\Omega}$ is an 8×8 matrix. Instead of constructing and diagonalizing $\mathbf{\Omega}$, the stability condition for the three instabilities can be found in another way. The RHF wave function is unstable when

$$E\big(\Phi^{\mathrm{RHF}}\big) - E\big(\Phi^{\mathrm{CDW,ASDW}}\big) \geqslant 0, \tag{3.3.1}$$

the equality corresponding to the instability threshold.

Putting the orbitals of broken symmetry in the form (3.1.17)–(3.1.19) into Slater determinant and applying Condon–Slater rules (using the fact that the near instability threshold λ is close to 0 which allows to use approximations $\sin\lambda \approx \lambda$, $\cos\lambda \approx 1 - (1/2)\lambda^2$ and to omit terms in power of λ higher than 2), we get the following instability conditions for CDW, ASDW$_1$ and ASDW$_2$ solutions:

$$\begin{aligned}
\text{CDW}: \quad & \varepsilon_{\pi^*_{xu(g)}} - \varepsilon_{\pi_{xg(u)}} + 3(\pi_{xg}\pi_{xu}|\pi_{xg}\pi_{xu}) - (\pi_{xg}\pi_{xg}|\pi_{xu}\pi_{xu}) \\
& - 4(\pi_{xg}\pi_{xu}|\pi_{yg}\pi_{yu}) + (\pi_{xg}\pi_{yu}|\pi_{yg}\pi_{xu}) + (\pi_{xg}\pi_{yg}|\pi_{xu}\pi_{yu}) \leqslant 0, \qquad (3.3.2) \\
\text{ASDW}_1: \quad & \varepsilon_{\pi^*_{xu(g)}} - \varepsilon_{\pi_{xg(u)}} - (\pi_{xg}\pi_{xu}|\pi_{xg}\pi_{xu}) - (\pi_{xg}\pi_{xg}|\pi_{xu}\pi_{xu}) \\
& + (\pi_{xg}\pi_{yu}|\pi_{yg}\pi_{xu}) + (\pi_{xg}\pi_{yg}|\pi_{xu}\pi_{yu}) \leqslant 0, \qquad (3.3.3) \\
\text{ASDW}_2: \quad & \varepsilon_{\pi^*_{xu(g)}} - \varepsilon_{\pi_{xg(u)}} - (\pi_{xg}\pi_{xu}|\pi_{xg}\pi_{xu}) - (\pi_{xg}\pi_{xg}|\pi_{xu}\pi_{xu}) \\
& - (\pi_{xg}\pi_{yu}|\pi_{yg}\pi_{xu}) - (\pi_{xg}\pi_{yg}|\pi_{xu}\pi_{yu}) \leqslant 0, \qquad (3.3.4)
\end{aligned}$$

where ε is an orbital energy, star denotes virtual orbital and the subscripts in parentheses correspond to Φ_2^{RHF}. The same conditions hold for π_y orbitals, these three instabilities are doubly degenerate.

As it can be seen in figures 1–3, conditions (3.3.2)–(3.3.4) are fulfilled even for the very short Fe–CH distances. The three instabilities leading to the broken-symmetry UHF solutions appear at the Fe–CH distance much shorter than the RHF equilibrium distance. Condition (3.3.4) is fulfilled as the first one. This leads to the ASDW$_2$ broken-symmetry wave function. This wave function in the dissociation limit has two carbon atoms with two electrons coupled to the triplet on p_x and p_y orbitals, which has the lowest energy on the HF level. The ASDW$_1$ instability, leading to singlet coupled carbon p_x and p_y electrons in the dissociation limit, appears as the second one. The CDW instability appears as the last one, with doubly occupied p_x (or p_y) carbon orbitals in the dissocitation limit and with the highest energy.

3.4. CAS calculations

We have performed three sets of CAS calculations for $Fe(CH)_2$, CAS(8,8) with eight electrons in eight active orbitals, CAS(10,10) with ten electrons in ten active orbitals and CAS(12,12) with twelve electrons in twelve active orbitals. CAS calculations have been done using the symmetry group D_{2h}. In all cases the energies of singlet, triplet and quintet wave functions have been calculated. In the case of CAS(12,12) quintet calculations the number of CSFs produced was too large, and we restricted the number of excitations to ten. In this case the wave function was not of the CAS type. We checked for singlet and triplet wave functions that this restriction does not influence calculated energy. As the starting orbitals for CAS calculations we have taken the natural orbitals from the $\Phi^{\mathrm{UHF(S)}}$ wave function. As the active space for CAS(8,8) we have taken $\Phi_3^{\mathrm{ASDW}_2}$ natural orbitals wiht occupation numbers between 1.28 and 0.73. They are π_{xg}, π_{xu}, π_{yg}, π_{yu} and four singly occupied Fe d orbitals (d_{z^2}, d_{xz}, d_{yz}, d_{xy}). For CAS(10,10) we have taken additionally σ_g and σ_g^* orbitals. The σ_u^* natural orbital of $\Phi_{\mathrm{UHF(S)}}$ has a smaller occupation number than σ_g^*. Even when starting CAS(10,10) with σ_u^* orbital it converted to σ_g^* during the iteration process. For CAS(12,12) we have added one σ_u and one σ_u^* orbital to the active space. We have performed CAS calculations wih basis set B_1 for three spin states, singlet, triplet and quintet. The energies and equilibrium Fe–CH distances for CAS wave functions are presented in table 3. The calculated energy separation between singlet and triplet is 2.5 kcal/mol for CAS(8,8), 3.1 kcal/mol for CAS(10,10) and 2.5 kcal/mol for CAS(12,12) with the singlet lying lower. We have repeated CAS calculations with basis set B_2 to see if the singlet–triplet ordering will be retained. The obtained singlet–triplet energy differences are approximately the same as for the smaller basis (2.5 kcal/mol for CAS(8,8), 3.1 kcal/mol for CAS(10,10) and 3.1 kcal/mol for CAS(12,12)). The occupation numbers of natural orbitals for CAS, $\Phi_3^{\mathrm{ASDW}_2}$ and $\Phi^{\mathrm{UHF(S)}}$ wave functions are shown in table 4. In all CAS calculations the d_{xz} and d_{yz} orbitals are almost evenly distributed between π_g and π_g^* CAS natural orbitals. The comparison of UHF and CAS natural orbital occupation numbers from table 4 show that UHF π_g occupation numbers are much lower and π_g^* much higher than respective CAS occupation numbers. Atomic orbital populations and charges for CAS wave functions are presented in table 5. From tables 1 and 3 it can be seen that the RHF wave functions yield the Fe–CH bond distance shorter and spatial and/or spin unrestricted HF wave functions yield this distance longer than CAS wave functions (with the exception of quintet wave function $\Phi^{\mathrm{RHF(Q)}}$). For both basis sets the lowest energy UHF wave function $\Phi^{\mathrm{UHF(S)}}$ has energy lower than the CAS(8,8) wave function. The explanation may be that the CAS(8,8) active space comprises four π orbitals and four singly occupied d Fe orbitals and takes into account non-dynamical correlation in this space, while $\Phi^{\mathrm{UHF(S)}}$ takes into account also some σ orbital correlation which is manifested by its σ orbitals occupation numbers.

Table 3
Fe–CH bond distances (R_{eq}) and energies for CAS wave functions of $Fe(CH)_2$.

Wave function	R_{eq} [Å]	E [a.u.]	$E - E$(S) [kcal/mol]
		Basis B_1	
CAS(8,8) (S)[a]	1.95	−199.350	0.0
CAS(8,8) (T)[b]	1.96	−199.346	2.5
CAS(8,8) (Q)[c]	1.98	−199.338	7.5
CAS(10,10) (S)	1.93	−199.366	0.0
CAS(10,10) (T)	1.94	−199.361	3.1
CAS(10,10) (Q)	1.95	−199.351	9.4
CAS(12,12) (S)	1.94	−199.371	0.0
CAS(12,12) (T)	1.94	−199.367	2.5
CAS(12,12) (Q)	1.96	−199.359	7.5
		Basis B_2	
CAS(8,8) (S)	1.94	−199.371	0.0
CAS(8,8) (T)	1.95	−199.367	2.5
CAS(8,8) (Q)	1.96	−199.358	8.2
CAS(10,10) (S)	1.92	−199.389	0.0
CAS(10,10) (T)	1.93	−199.384	3.1
CAS(10,10) (Q)	1.94	−199.373	10.0
CAS(12,12) (S)	1.93	−199.407	0.0
CAS(12,12) (T)	1.93	−199.402	3.1
CAS(12,12) (Q)	1.95	−199.390	10.7

[a] S – singlet; [b] T – triplet; [c] Q – quintet.

Table 4
Natural orbital occupation numbers for CAS wave functions and for $\Phi_3^{ASDW_2}$ and $\Phi^{UHF(S)}$.

Wave function	Natural orbital occupation numbers											
	σ_u	σ_g	π_{xg}	π_{yg}	π_{xu}	π_{yu}	d_{xy}	d_{z^2}	π^*_{xg}	π^*_{yg}	σ^*_g	σ^*_u
						Basis B_1						
CAS(12,12) (S)	1.981	1.971	1.471	1.471	0.999	0.999	1.000	1.000	0.530	0.530	0.037	0.011
CAS(12,12) (T)	1.981	1.971	1.446	1.446	1.000	1.000	1.000	1.000	0.555	0.555	0.036	0.011
CAS(12,12) (Q)	1.981	1.974	1.382	1.382	1.000	1.000	1.000	1.000	0.618	0.618	0.034	0.010
$\Phi_3^{ASDW_2}$	1.994	1.982	1.188	1.188	1.000	1.000	1.000	1.000	0.811	0.811	0.018	0.006
$\Phi^{UHF(S)}$	1.994	1.982	1.278	1.278	1.000	1.000	1.000	1.000	0.721	0.721	0.018	0.006
						Basis B_2						
CAS(12,12) (S)	1.981	1.970	1.467	1.467	0.999	0.999	1.000	1.000	0.534	0.534	0.037	0.011
CAS(12,12) (T)	1.981	1.971	1.441	1.441	1.000	1.000	1.000	1.000	0.560	0.560	0.036	0.010
CAS(12,12) (Q)	1.982	1.973	1.378	1.378	1.000	1.000	1.000	1.000	0.622	0.622	0.034	0.010
$\Phi^{UHF(S)}$	1.993	1.981	1.277	1.277	1.000	1.000	1.000	1.000	0.723	0.723	0.019	0.007

Table 5
Orbital populations on iron atom and charges for CAS wave functions of $Fe(CH)_2$.

Wave function	Atomic orbital populations on Fe[a]									Charges		
	d_{z^2}	d_{x^2}	d_{y^2}	d_{xz}	d_{yz}	d_{xy}	s	p	d_{total}	Fe	C	H
						Basis B_1						
CAS(8,8) (S)	0.76	1.13	1.13	1.11	1.11	1.00	0.58	0.06	6.24	1.12	−0.70	0.14
CAS(8,8) (T)	0.77	1.13	1.13	1.11	1.11	1.00	0.57	0.06	6.25	1.14	−0.71	0.14
CAS(8,8) (Q)	0.78	1.13	1.13	1.08	1.08	1.00	0.55	0.07	6.20	1.18	−0.74	0.15
CAS(10,10) (S)	0.75	1.13	1.13	1.12	1.12	1.00	0.62	0.04	6.25	1.11	−0.69	0.13
CAS(10,10) (T)	0.75	1.13	1.13	1.11	1.11	1.00	0.62	0.02	6.23	1.10	−0.69	0.14
CAS(10,10) (Q)	0.77	1.13	1.13	1.10	1.10	1.00	0.61	0.06	6.23	1.12	−0.70	0.14
CAS(12,12) (S)	0.75	1.13	1.13	1.12	1.12	1.00	0.65	0.05	6.25	1.06	−0.67	0.14
CAS(12,12) (T)	0.75	1.13	1.13	1.12	1.12	1.00	0.65	0.06	6.25	1.06	−0.67	0.14
CAS(12,12) (Q)	0.77	1.13	1.13	1.10	1.10	1.00	0.63	0.07	6.23	1.07	−0.68	0.14
						Basis B_2						
CAS(8,8) (S)	0.63	1.11	1.11	1.10	1.10	1.00	0.66	0.07	6.05	1.25	−0.74	0.12
CAS(8,8) (T)	0.63	1.11	1.11	1.09	1.09	1.00	0.66	0.08	6.03	1.25	−0.74	0.12
CAS(8,8) (Q)	0.64	1.11	1.11	1.08	1.08	1.00	0.65	0.08	6.02	1.27	−0.75	0.12
CAS(10,10) (S)	0.58	1.10	1.10	1.11	1.11	1.00	0.75	0.05	6.00	1.23	−0.73	0.11
CAS(10,10) (T)	0.60	1.10	1.10	1.10	1.10	1.00	0.72	0.06	6.00	1.25	−0.74	0.11
CAS(10,10) (Q)	0.61	1.10	1.10	1.09	1.09	1.00	0.70	0.07	5.99	1.26	−0.74	0.12
CAS(12,12) (S)	0.58	1.10	1.10	1.10	1.10	1.00	0.75	0.06	5.98	1.23	−0.72	0.11
CAS(12,12) (T)	0.57	1.10	1.10	1.10	1.10	1.00	0.74	0.07	5.97	1.22	−0.72	0.11
CAS(12,12) (Q)	0.60	1.10	1.10	1.09	1.09	1.00	0.73	0.09	5.98	1.22	−0.73	0.11

[a] Populations on s and p valence orbitals were summed up.

4. Conclusions

Our calculations have showed that there are many HF wave functions for linear $Fe(CH)_2$. The RHF wave functions are unstable. The symmetry breaking in π orbitals leads to HF solutions of CDW and ASDW type. These solutions have spatial and spin symmetry broken. There are also solutions with spatial symmetry preserved, but spin symmetry uncorrect like $\Phi^{\text{UHF(S)}}$. Comparing the Fe–CH distance obtained from various HF wave functions with CAS results, one can see that the RHF wave functions yield this distance too short, and symmetry and/or spin broken wave functions give it too long (tables 1 and 3). The broken-symmetry wave functions tend to overestimate the correlation effects, which is reflected in the longer bond distance and much smaller σ_g and π_g natural orbitals occupation numbers than those for CAS wave functions.

The existence of multiple instabilities in RHF wave functions is an indication of a large non-dynamic correlation in this system and the need for use of multireference wave function to describe it. The UHF natural orbitals can make a good starting guess for choosing the CAS active space orbitals. This method of choosing active space orbitals is a well-known UNO-CAS method [9].

References

[1] H. Ågren, P.S. Bagus and B.O. Roos, Chem. Phys. Lett. 82 (1981) 505.
[2] P.K. Baker, G.K. Barker, D.S. Gill, M. Green, A.G. Orpen, I.D. Williams and A.J. Welch, J. Chem. Soc. Dalton Trans. (1989) 1321.
[3] L.A. Barnes and R. Lindh, Chem. Phys. Lett. 223 (1994) 207.
[4] M. Bénard, J. Chem. Phys. 71 (1979) 571.
[5] M. Bénard, Theoret. Chim. Acta 61 (1982) 379.
[6] M. Bénard, Chem. Phys. Lett. 96 (1983) 18.
[7] A. Benchini and D.J. Gatteschi, J. Am. Chem. Soc. 108 (1986) 6763.
[8] R.C. Binning, Jr. and L.A. Curtiss, J. Comput. Chem 11 (1990) 1206.
[9] J.M. Bofill and P. Pulay, J. Chem. Phys. 90 (1989) 3637.
[10] M.C. Böhm, Mol. Phys. 46 (1982) 683.
[11] M.C. Böhm, J. Phys. B 16 (1983) L397.
[12] M.C. Böhm, J. Chem. Phys. 80 (1984) 2704.
[13] M.C. Böhm, J. Chem. Phys. 81 (1984) 855.
[14] M.C. Böhm, Z. Phys. B 56 (1984) 99.
[15] M. Bottrill, M. Green, A.G. Orpen, D.R. Saunders and I.D. Williams, J. Chem. Soc. Dalton Trans. (1989) 511.
[16] R. Broer-Bramm and W.C. Nieuwpoort, Chem. Phys. 54 (1981) 291.
[17] M.A. Buijse and E.J. Baerends, J. Chem. Phys. 93 (1990) 4129.
[18] M.A. Buijse and E.J. Baerends, Theoret. Chim. Acta 79 (1991) 389.
[19] B.E. Bursten, J.R. Jensen, D.J. Gordon, P.M. Treichel and R.F. Fenske, J. Am. Chem. Soc. 103 (1981) 5226.
[20] J.-L. Calais, Adv. Quantum Chem. 17 (1985) 225.
[21] J.T. Carter and D.B. Cook, J. Chem. Soc. Chem. Commun. (1987) 1672.
[22] G. Chambaud, B. Levy and P. Millie, Theoret. Chim. Acta 48 (1978) 103.
[23] D.B. Cook, Int. J. Quantum Chem. 34 (1992) 197.
[24] T.H. Dunning, Jr. and P.J. Hay, in: *Methods of Electronic Structure Theory*, ed. H.F. Schaefer III (Plenum Press, New York, 1977) chapter 1.
[25] M. Dupuis, D. Spangler, J.J. Wendoloski (NRCC Staff), M.W. Schmit (North Dakota University) and S.T. Elbert (Iowa State University), *GAMESS*, Version 22 February (1995).
[26] A.C. Fillipou, Polyhedron 9 (1990) 727.
[27] A.C. Fillipou, W. Grünleitner, C. Völkl and P. Kiprof, Angew. Chem. 103 (1991) 1188.
[28] H. Fukutome, Progr. Theoret. Phys. 50 (1973) 1433.
[29] H. Fukutome, Progr. Theoret. Phys. 52 (1974) 1766.
[30] H. Fukutome, Int. J. Quantum Chem. 20 (1981) 955.
[31] J.T. Golab, D.L. Yeager and P. Jorgensen, Chem. Phys. 93 (1985) 83.
[32] A. Goursot, J.P. Malrieu and D.R. Salahub, Theoret. Chim. Acta 91 (1995) 225.
[33] M.F. Guest, I.H. Hillier, A.A. MacDowell and M. Berry, Mol. Phys. 41 (1980) 519.
[34] J.R. Hart, A.K. Rappé, S.M. Gorun and T.H. Upton, Inorg. Chem. 31 (1992) 5254.
[35] P.J. Hay, J. Chem. Phys. 66 (1977) 4377.
[36] P.J. Hay and W.R. Wadt, J. Chem. Phys. 82 (1985) 299.
[37] M. Jaworska, P. Lodowski and J. Nowakowski, Chem. Phys. Lett. 232 (1995) 328.
[38] U. Kaldor, Chem. Phys. Lett. 185 (1991) 131.
[39] M.B. Lepetit and J.P. Malrieu, Chem. Phys. Lett. 169 (1990) 285.
[40] M.B. Lepetit, J.P. Malrieu and M. Péllisier, Phys. Rev. A 39 (1989) 981.
[41] M.B. Lepetit, J.P. Malrieu and G. Trinquier, Chem. Phys. 130 (1989) 229.
[42] M.B. Lepetit, M. Pélissier and J.P. Malrieu, J. Chem. Phys. 89 (1988) 998.
[43] X. Li and J. Paldus, J. Chem. Phys. 102 (1995) 2013.
[44] C. Liang and H.F. Schaefer III, Chem. Phys. Lett. 169 (1990) 150.

[45] T. Lovell, J.E. McGrady, R. Strange and S.A. Macgregor, Inorg. Chem. 35 (1996) 3079.
[46] P.O. Löwdin, Phys. Rev. 97 (1955) 1509.
[47] J. Manna, S.J. Geib and M.D. Hopkins, Angew. Chem. 105 (1993) 897.
[48] A. Mayr and C.M. Bastos, J. Am. Chem. Soc. 112 (1990) 7797.
[49] M.H. McAdon and W.A. Goddard III, J. Chem. Phys. 88 (1988) 277.
[50] M.H. McAdon and W.A. Goddard III, J. Chem. Phys. 92 (1988) 1352.
[51] G.A. Medley and R. Stranger, Inorg. Chem. 33 (1994) 3976.
[52] M. Merchán, R. Pou-Amérigo and B.O. Roos, Chem. Phys. Lett. 252 (1996) 405.
[53] M.M. Mestechkin, *Instability of Hartree–Fock Solutions and Molecular Stability* (Naukova Dumka, Kiev, 1986) (in Russian).
[54] J.-M. Mouesca, J.L. Chen, L. Noodleman, D. Bashford and D.A. Case, J. Am. Chem. Soc. 116 (1994) 11898.
[55] P. Mougenot, J. Demuynck and M. Bénard, J. Phys. Chem. 92 (1988) 571.
[56] L. Noodleman, J. Chem. Phys. 74 (1981) 5737.
[57] L. Noodleman and E.J. Baerends, J. Am. Chem. Soc. 106 (1984) 2316.
[58] L. Noodleman and D.A. Case, Adv. Inorg. Chem. 38 (1992) 423.
[59] L. Noodleman, D.A. Case and A. Aizman, J. Am. Chem. Soc. 110 (1988) 1001.
[60] L. Noodleman and E.R. Davidson, Chem. Phys. 109 (1986) 131.
[61] M. Ozaki and H. Fukutome, Progr. Theoret. Phys. 60 (1978) 1322.
[62] J. Paldus, Hartree–Fock stability and symmetry breaking, in: *Self-Consistent Field: Theory and Applications*, eds. R. Carbo and M. Klobukowski (Elsevier, New York, 1990).
[63] J. Paldus, E. Chin and M.G. Grey, Int. J. Quantum Chem. 14 (1983) 395.
[64] J. Paldus and J. Čižek, J. Chem. Phys. 47 (1967) 3976.
[65] J. Paldus and J. Čižek, J. Chem. Phys. 52 (1970) 2919.
[66] J. Paldus and J. Čižek, J. Chem. Phys. 53 (1970) 821.
[67] J. Paldus and J. Čižek, Phys. Rev. A 2 (1970) 2268.
[68] J. Paldus and J. Čižek, J. Chem. Phys. 54 (1971) 2293.
[69] J. Paldus and J. Čižek, Phys. Rev. A 3 (1971) 525.
[70] R. Pauncz and J. Paldus, Int. J. Quantum Chem. 14 (1983) 411.
[71] A.J.L. Pombeiro and L.R. Richards, Transition Met. Chem. 5 (1980) 55.
[72] P.K. Ross and E.I. Solomon, J. Am. Chem. Soc. 113 (1991) 3246.
[73] J.C. Slater, Phys. Rev. 82 (1951) 538.
[74] J.F. Stanton, J. Gauss and R.J. Bartlett, J. Chem. Phys. 97 (1992) 5554.
[75] M. Takahashi, J. Paldus and J. Čižek, Int. J. Quantum Chem. 14 (1983) 707.
[76] K. Takatsuka, T. Fueno and K. Yamaguchi, Theoret. Chim. Acta 48 (1978) 175.
[77] T.E. Taylor and M.B. Hall, Chem. Phys. Lett. 114 (1985) 338.
[78] R. Wiest and M. Bénard, Theoret. Chim. Acta 66 (1984) 65.
[79] K. Yamaguchi, Chem. Phys. 25 (1977) 215.
[80] K. Yamaguchi, Int. J. Quantum Chem. 12 (1982) 459.
[81] K. Yamaguchi, Instability in chemical bonds – SCF, APUMP, APUCC, MR-CI and MR-CC approaches, in: *Self-Consistent Field: Theory and Applications*, eds. R. Carbo and M. Klobukowski (Elsevier, New York, 1990).
[82] K. Yamaguchi, T. Fueno, N. Ueyama and A. Nakamura, Chem. Phys. Lett. 164 (1989) 211.
[83] K. Yamaguchi, Y. Takahara, T. Fueno and K.N. Houk, Theoret. Chim. Acta 73 (1988) 337.
[84] K. Yamaguchi, T. Tsunekawa, Y. Toyoda and T. Fueno, Chem. Phys. Lett. 143 (1988) 371.
[85] K. Yamaguchi, Y. Yoshioka, T. Takatsuka and T. Fueno, Theoret. Chim. Acta 48 (1978) 185.